CoFlex TOP: A teleoperation system for flexible ureteroscopy*

Christopher Schlenk[1], Anja Hellings-Kuß[1], Katharina Hagmann[1], Nikola Budjakoski[1], Laura Oliva Maza[1], Julian Klodmann[1], Sebastian Müller-Spahn[1], Florian Steidle[1], Arkadiusz Miernik[2] and Alin Albu-Schäffer[1]

***Abstract*—In flexible ureteroscopy (fURS) for kidney stones, the renal collecting system is inspected and stones are removed with a flexible ureteroscope (FU). One alternative to the fragmentation of stones and their removal with the help of graspers or extraction baskets is the dusting of stones with laser light. To support a single surgeon during a fURS procedure, in particular with the fine manipulation during dusting, we developed the *CoFlex TOP* system for the teleoperation of a handheld FU with three degrees of freedom. This paper describes the overall structure of the system, its kinematics and the hardware and software components. Subsequently, the system properties and its position repeatability are investigated and the system's feasibility for a tip positioning task in virtual reality is evaluated in a user study. Finally, we discuss the implications of the evaluation and sketch possible foci of a user study with urology surgeons.**

***Index Terms*—Medical Robots and Systems; Telerobotics and Teleoperation; Performance Evaluation and Benchmarking**

I. Introduction

KIDNEY stones (or renal calculi) are solid accumulations of minerals, salts and organic material that form within the kidneys. They affect patients worldwide: 7-13% of the population in North America, 5-9% in Europe, and 1-5% in Asia experience kidney stones during their lifetime [1]. The treatment options depend on the size, location and composition of the stones as well as on habitus and renal anatomy of the patient. Larger kidney stones or stones blocking the urinary tract are typically treated by extracorporeal shock wave lithotripsy (40-50% worldwide use), ureteroscopy (30-40%) or percutaneous nephrolithotomy (5-10%) [2], [3].

In ureteroscopy, an ureteroscope (endoscope for the urinary tract) is advanced through the urinary tract to the stone location. An ureteral access sheath can be used to protect the urinary tract from lesions. Distal ureteral stones can be treated with (semi)rigid ureteroscopes, but stones in the kidney calyces require flexible ureteroscopes (FU), whose tip is bendable at one degree of freedom (DoF). Ureteroscopy with FUs is called flexible ureteroscopy (fURS). Larger stones are fragmented with laser light from a flexible fiber in the FU working channel before the fragments are grasped. Smaller stones are directly grasped using forceps or an extraction basket. An alternative to stone fragmentation is stone dusting by laser. To reduce the kidney stones to small particles, which can pass with the urinary flow, the surgeon continuously moves the laser tip either circumferentially along the edges of the stone or in a meandering path from one leading edge towards the center of the stone [4]. This motion requires precise, incremental pose changes of the FU tip. Dusting may gain more importance compared to stone fragmentation in the future, as new Thulium fiber lasers allow higher stone ablation rates resulting in shorter procedures [5].

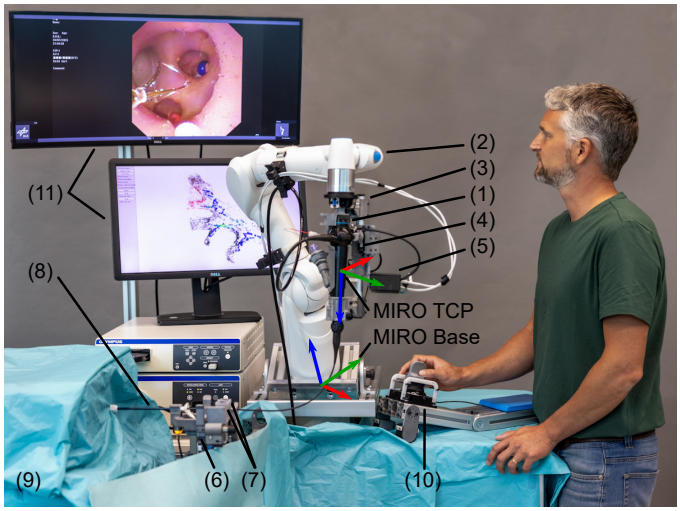

Fig. 1. Test setup for the teleoperation system *CoFlex TOP*. The flexible ureteroscope (FU, (1)) is docked to the tool interface of the DLR MIRO (2) via the *Robot Side Unit* (RSU, (3)). The servomotor for the FU tip bending (4) actuates the lever at the FU handle. A microcontroller (5) processes the data from the RSU sensors. The FU shaft is inserted into the *Patient Side Unit* (PSU, (6)) with its two translationally and rotationally movable rollers (7). An ureteral access sheath (8) guides the FU shaft from the PSU to the operation field over the field generator of the electromagnetic tracking (9). The user teleoperates the system with the hand controller (10) while receiving visual feedback via two displays (11).

Performing a fURS procedure poses different challenges to the surgeons:

- **X-ray exposure**: fluoroscopic imaging is the standard intraoperative imaging method in fURS [3]. The surgeon holding the FU is located close to the X-ray unit and thus must wear a lead vest.
- **Need for second surgeon**: the manual handling of

Manuscript received: September, 13, 2023; Revised January, 14, 2024; Accepted February, 25, 2024.

This paper was recommended for publication by Jee-Hwan Ryu upon evaluation of the Associate Editor and Reviewers' comments.

[1] These authors are with the Institute of Robotics and Mechatronics, DLR, Oberpfaffenhofen, Germany julian.klodmann@dlr.de

[2] This author is with the Department of Urology, University of Freiburg, Freiburg, Germany

This paper has supplementary downloadable material available at http://ieeexplore.ieee.org, provided by the authors. This includes one video clip without audio describing the CoFlex TOP system (size 39.9 MB).

Digital Object Identifier (DOI): see top of this page.

flexible ureteroscopes requires two surgeons. The first surgeon holds the handle of the FU in one hand and its shaft in the other (see Fig. 4 left), the second surgeon operates the active irrigation, laser fiber and extraction basket. Intervention steps like lasering or stone grasping thus require a good coordination of both surgeons.

- **Unergonomic body postures**: as both surgeons interact directly with the FU, they must position themselves between the spread legs of the patient. This imposes unergonomic body postures, which can lead to musculoskeletal problems. In a study among 285 urologists, 62.1% of them reported such disorders [6].
- **Unergonomic hand postures**: the manual FU manipulation strongly strains the hand at the FU handle. As apparent in Fig. 4 left, it must hold the weight of the FU handle and perform large wrist movements to rotate the FU shaft. At the same time, its thumb must precisely move the handle lever to bend the FU tip. Hand or wrist injuries are common consequences, e.g. reported by 32% of 122 interviewed endourologists in [7].

To support the surgeons with these challenges, in particular with the fine manipulation of the FU tip pose during dusting, we extended the previously developed system for robot-supported fURS by a single surgeon [8], [9] to the teleoperation system *CoFlex TOP* displayed in Fig. 1. For a detailed description of the contributions, please see subsection III-C.

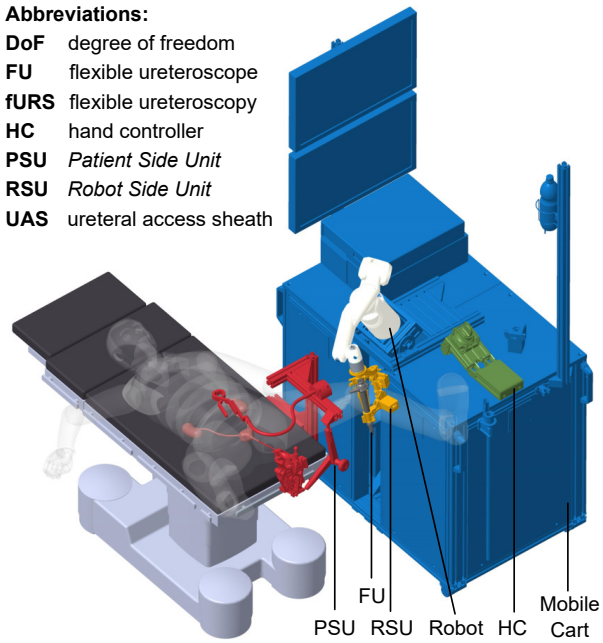

Fig. 2. Proposed operating room setup for *CoFlex TOP*: the robot arm (white) is mounted on a mobile cart (blue), which is positioned beside the operating table with the patient. The RSU (orange) at the tool interface of the robot allows the attachment of the flexible ureteroscope (grey). The PSU (red) is attached to the side rail of the operating table. The hand controller (green) can be positioned according to the preferences of the surgeon.

II. State of the Art

The existing systems for the manipulation of flexible endoscopes can be classified into attachable actuation units and robotic telemanipulation systems (compare [9]).

Attachable actuation units actuate some or all DoFs at the endoscope handle. They can be either hand-held [10] or mounted on a passive arm [11], [12], [13], [14], [15]. They are compact, but hand-held systems increase the weight carried by the surgeon. Systems mounted on a passive arm allow either no or only a limited motorized repositioning of the endoscope handle. The manual repositioning of the endoscope handle, which is regularly required in fURS, is cumbersome in such systems: the combined weight of endoscope, actuation unit and passive arm must be handled, while the passive arm restricts the motion capabilities.

Telemanipulation systems for ureteroscopy as presented in [16], [17], [18], [19], [20] provide full weight compensation and allow the teleoperation of the endoscope from a remote surgeon console. However, the combined footprint of the robot cart with the FU and the surgeon console is large. Additionally, a second person at the operating table is required to insert the ureteroscope into the urinary tract of the patient and exchange laser fibers or extraction baskets. An intraoperative conversion to manual fURS is complex and requires sterile clothing of the surgeon, removing the robot cart from the patient and undocking the FU from the robot.

III. Concept of the Teleoperation System

Based on the challenges in manual fURS and the shortcomings of existing actuation units and telemanipulation systems, we identified the following three development goals for a robotic system to support fURS:

1) **Use existing operating room equipment**: the system shall allow integration of existing FUs, laser fibers, baskets and accessories like ureteral access sheaths.
2) **Allow whole fURS intervention by one surgeon**: the system shall enable a single surgeon to perform fURS. This would save staff and cost, avoid communication errors and extend the elbowroom of the surgeon.
3) **Comply with existing surgical workflows**: for each intervention phase the system should provide the adequate degree of robotic support, imposing a low system utilization entry threshold. Additionally, the surgeon shall always have the fallback option of manual fURS.

A. System structure

To achieve these goals, we propose the operating room setup in Fig. 2 for the teleoperation system *CoFlex TOP*.

The surgeon attaches the FU handle via the *Robot Side Unit* (RSU) to the tool interface of a versatile lightweight robot DLR MIRO. For more details about the robot and its control interfaces please refer to [8]. The RSU contains a motor for actuating the FU tip bending, denoted as θ in Fig. 4. The robot compensates the weight of the FU handle while it is attached. Thus, the surgeon can use both hands to e.g. insert a laser fiber or an extraction basket into the working channel of the FU. The robot, the FU light source and video processing unit, the control PCs of the robotic system, the displays for the endoscope image, the laser source and the irrigation pump are integrated into a mobile cart (for more details please see [9]).

The patient is positioned on the operating table as in manual fURS with his/her spread legs pointing upwards (lithotomy position). Attached to the standardized side rails of the operating table is the *Patient Side Unit* (PSU). It provides a fixture for the ureteral access sheath, which is inserted into the urinary tract of the patient. The pose of the thereby fixated entrance to the urinary tract with respect to the robot is registered using a disposable registration probe, which is temporarily attached to the RSU (for more details, please see [8]). Based on this registration, the motion range of the robotic arm is limited while the FU shaft is inserted into the ureteral access sheath to prevent excessive pulling on the flexible shaft. The PSU contains two motors for actuating the FU tip translation and rotation (z and ψ in Fig. 4).

In teleoperation, the surgeon controls the movements of the FU tip via a hand controller (Fig. 4 right). This hand controller can be positioned according to the surgeon's preferences, e.g. on the mobile cart.

B. Hybrid surgery workflow

The workflow in Fig. 3 displays the basic concept of the *CoFlex TOP* system: depending on the surgical task, the surgeon adapts the degree of robotic support between none (*Manual Surgery*), *Solo Surgery*, and *Teleoperation*. The transitions between the three support degrees shall be quick and require no tools.

In *Solo Surgery* mode, the robot compensates the weight of the FU handle while the surgeon manually positions it and maintains the handle pose, when the surgeon releases it. Thus, one surgeon can perform a complete fURS intervention (compare the user study with urology surgeons in [9]). All DoF of the FU are actuated manually by the surgeon in this mode. This ensures unaltered haptic feedback from the operation site but does not allow to enhance precision, e.g. by telemanipulation or automated motion of the FU tip.

In *Teleoperation* mode, the robot with the attached FU handle follows the translations and rotations of the FU shaft (z and ψ in Fig. 4 left). Additionally, all DoF of the FU are teleoperated according to the user inputs at the hand controller. This unburdens the surgeon from the direct actuation of the FU handle. For fine manipulation tasks such as stone dusting, a motion scaling can be implemented.

C. Contribution

The two previous publications [8], [9] focused on the *Solo Surgery* system, thus mainly addressing the development goals 1) and 2) in section III. This paper introduces in section IV the extensions to the *Solo Surgery* system, which enable the robotic teleoperation of the FU. The resulting *CoFlex TOP* system also addresses the third development goal: it enables quick and tool-free transitions between the three support degrees. At the same time, it supports fine manipulation in fURS as e.g. required during dusting. The evaluation of both the system's technical properties and its potential for fine manipulation are described in section V and discussed in section VI. In detail, the contributions of this paper are:

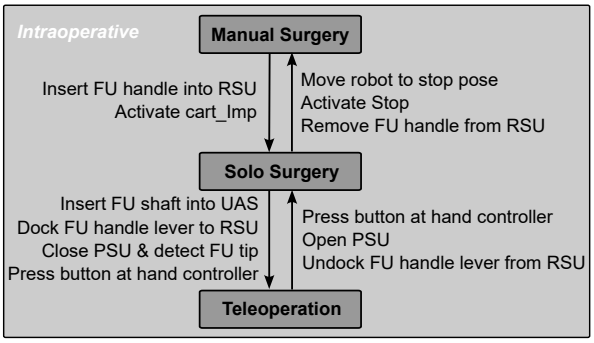

Fig. 3. The proposed hybrid surgery workflow for the *CoFlex TOP* system: the surgeon switches depending on the current task intraoperatively between *Manual Surgery*, *Solo Surgery* (see [9]), and *Teleoperation*. The system design supports a quick change of the three operation modes.

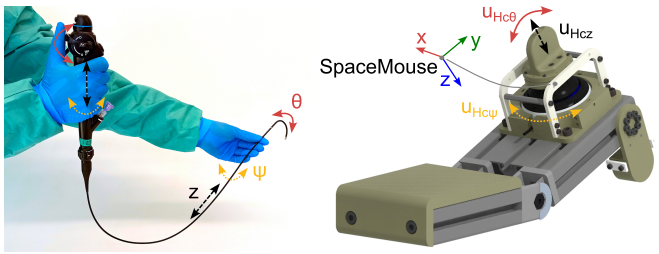

Fig. 4. Motion mapping for manual handling (left) and teleoperation of the FU (right): for manual handling, the surgeon controls the tip bending with the lever at the FU handle (continuous red arrows), the rotation around the shaft axis by rotating both handle and shaft (dotted yellow arrows) and the translation along the shaft axis by translating both handle and the flexible shaft close to the patient access (black dashed arrows). In teleoperation, the FU tip is bent by tilting around the *SpaceMouse* x-axis (red arrow), the FU shaft rotated by rotating around the *SpaceMouse* z-axis (yellow arrow) and the FU shaft translated by pushing/pulling along the z-axis (black arrow).

- Adaptations of the RSU hardware and the modular software architecture for teleoperation;
- Design of a hand controller for teleoperation of FUs;
- Design of a novel drive concept for flexible medical shafts (for the PSU) and evaluation of its position repeatability and slip detection concept;
- Kinematics of the developed teleoperation system;
- User study comparing manual and teleoperated fine manipulation of the FU tip.

IV. Design of the Teleoperation System

The following subsections describe in greater detail the hardware architecture, the kinematics and the software architecture of *CoFlex TOP*.

A. Hardware architecture

CoFlex TOP enhances earlier developments [8], [9] and features the same basic structure with RSU at the robot and PSU at the operating table.

The tip motion of the flexible ureteroscope *Olympus URF-V*[1] is controlled by a hand controller based on a *SpaceMouse Compact*[2] (see Fig. 4 right). As only three of the six DoF of

[1]Olympus Deutschland GmbH, Hamburg, Germany
[2]3Dconnexion GmbH, Munich, Germany

the *SpaceMouse Compact* are required to move the tip, the hand controller structure obstructs lateral movements.

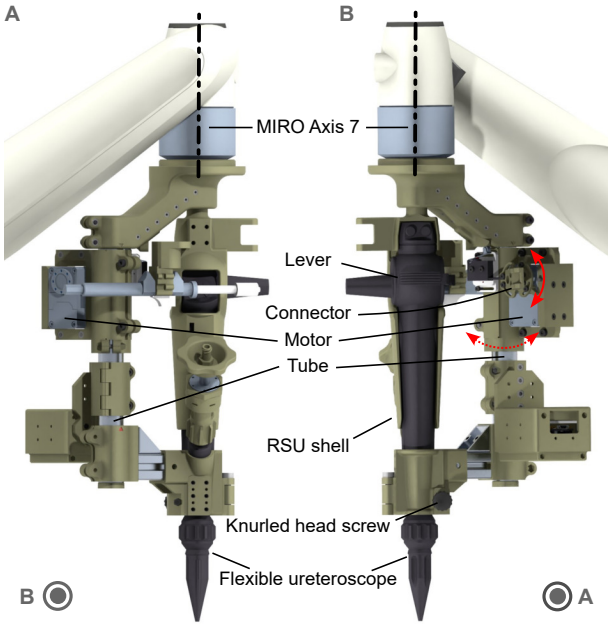

Fig. 5. The RSU at the DLR MIRO with attached flexible ureteroscope: after the FU handle has been clamped in the RSU shell by turning the knurled head screw, the motor for tip bending can be rotated around the aluminum tube till the connector clasps the lever (dotted red arrow). Then the motor can actuate the lever (solid red arrow).

Within the RSU displayed in Fig. 5, a servomotor *Dynamixel XH430-W210-R* replaced the position encoder for the FU handle lever. This servomotor (as well as the two servomotors in the PSU) is controlled using a motor controller *U2D2* and a *U2D2 power hub*[3]. The RSU shell integrates two capacitive sensors to detect the grasping and releasing by the surgeon and two buttons to control the irrigation. Sensors and buttons are read out by a microcontroller *Arduino Micro*[4].

The actuation principle of the PSU is sketched in Fig. 6. The rotation of cylindrical rollers around their longitudinal axes actuates the shaft translation. The synchronous, reverse translation of the rollers along their longitudinal axes actuates the shaft rotation. This actuation principle allows for a compact and simple design with a well defined cable guidance and an easy separation of FU and PSU.

The PSU is equipped with two waterproof servomotors *Dynamixel XW430-T200-R*. As displayed in Fig. 7, the servomotor for the shaft rotation (1) turns a tooth gear. The tooth gear moves via two gear racks two carts on two miniature profiled rail guides. This results in a reverse translation of the two rollers. The second servomotor (6) turns the roller (3) to actuate the shaft translation. The roller (2) is equipped with a rotary magnetic encoder *AS5600* (7). By comparing the positions of the shaft translation servomotor and the measurements of the position encoder, slip between the motor roller and the FU shaft can be detected. Roller (2) is pressed against the FU shaft by a compression spring *Gutekunst VD-143B*[5]. This establishes a frictional connection between the two rollers and the FU shaft. Roller (2) can be removed from the FU shaft and fixated in the removed position by pressing the knob of the locking indexing plunger *Ganter GN 514*[6] (10). This way, the FU shaft is not connected anymore and the surgeon can move it manually while receiving haptic feedback.

The inductive sensor *Omron E2B-M18KN16-WP-B1 2M*[7] (8) detects, when the FU tip enters/leaves the *Flexor Ureteral Access Sheath FUS-120035*[8] (9). Thus, the relation between the positions of FU tip, shaft translation motor and position encoder can be established and if necessary updated.

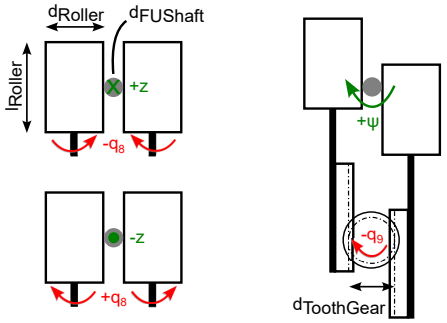

Fig. 6. The actuation principle of the PSU: the rotation q_8 of the rollers with diameter d_{Roller} and length l_{Roller} around their axes induces a translation of the FU shaft with diameter $d_{FUShaft}$ (left). The synchronous, reverse translation of the rollers along their axes due to the rotation q_9 of the tooth gear with diameter $d_{ToothGear}$ induces a rotation of the FU shaft around its axis (right).

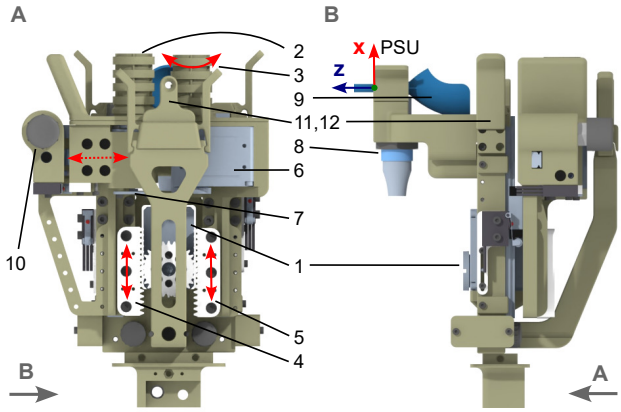

Fig. 7. Frontal (A) and side view (B) of the PSU with the red arrows indicating the possible actuated (solid arrow) and manual motions (dotted arrow) of the components: the servomotor for the shaft rotation (1) drives the translation of the rollers (2, 3) via two gear racks (4, 5). The servomotor for the shaft translation (6) actuates the FU shaft translation into the patient. The spring-pretensioned roller (2) ensures contact between FU shaft and driven roller (3) and is connected to an encoder (7) for slip detection. The inductive sensor (8) detects when the FU tip enters/leaves the ureteral access sheath (9). A locking indexing plunger (10) can fixate roller (2) in the detached position. Two guides (11, 12) ensure a defined position of the FU shaft.

B. Kinematics

The mapping of the servomotors for shaft translation (q_8), shaft rotation (q_9) and tip bending (q_{10}) to the FU tip pose is

[3]all ROBOTIS Co., Seoul, South Korea
[4]Arduino Srl, Monza, Italy
[5]Gutekunst + Co.KG, Metzingen, Germany
[6]Otto Ganter GmbH & Co. KG, Furtwangen, Germany
[7]Omron Electronics GmbH, Langenfeld, Germany
[8]CookMedical Inc., Bloomington, IN, USA

described for the motor angles in radians by:

$$\begin{pmatrix} z(t) \\ \psi(t) \\ \theta(t) \end{pmatrix} = \begin{pmatrix} -\frac{d_{Roller}}{2} q_8 \\ -\frac{d_{ToothGear}}{d_{FUShaft}} q_9 \\ k_b q_{10} \end{pmatrix}.$$

Each motor influences one DoF of the FU tip. Due to torsional stiffness of the FU shaft, for changing ψ a simultaneous rotation of the FU handle around the MIRO axis 7 (see Fig. 5) and a translation of the PSU rollers is necessary to prevent twisting of the shaft. The shaft translation z and the shaft rotation ψ depend on the geometry of rollers, shaft and tooth gear (compare Fig. 6) with d_{Roller} = 27.0 mm, $d_{FUShaft}$ = 3.3 mm and $d_{ToothGear}$ = 30 mm. The maximum translation speed in z-direction with ω_{8max}=53 rev/min at 12 V supply voltage is 74.9 mm/s.

The output angle q_{10} of the servomotor for tip bending is directly transmitted to the lever at the FU handle as displayed in Fig. 5. For the *Olympus URF-V*, the motion range of the handle lever is about 71° while the tip motion range is 455°. Consequently, the scaling function can be linearly approximated by $k_b = \frac{455°}{71°} = 6.4$.

The position resolution and the backlash of the bending servomotor limits under this assumption the maximum (theoretical) rotational FU tip accuracy to 2.2°. The exact mapping between q_{10} and θ, however, displays a significant hysteresis and depends on the internal friction and elasticities of the FU as well as on external loads on its tip.

C. Software architecture

The modular software architecture from [9] was extended for *CoFlex TOP* by adding the green components in Fig. 8: an additional control model *Uri control* for the three servomotors in PSU and RSU was implemented in *MATLAB Simulink*[9]. For the teleoperation of the FU an additional control mode top_{posIF} was integrated into *Uri control* and *MIRO control*. When it is activated by pressing button *BS2* at the *SpaceMouse*, the $q_{des} \in \mathcal{R}^{3x1}$ for the three servomotors is calculated from the user inputs at the hand controller as:

$$\mathbf{q_{des}}(t) = \mathbf{q_{des}}(t-1) + \mathbf{\Delta q} = \mathbf{q_{des}}(t-1) + \mathbf{k} \cdot \mathbf{u_{Hc}}(t),$$

$$\begin{pmatrix} q_{8des}(t) \\ q_{9des}(t) \\ q_{10des}(t) \end{pmatrix} = \begin{pmatrix} q_{8des}(t-1) \\ q_{9des}(t-1) \\ q_{10des}(t-1) \end{pmatrix} + \begin{pmatrix} k_8 \cdot u_{Hcz}(t) \\ k_9 \cdot u_{Hc\psi}(t) \\ k_{10} \cdot u_{Hc\theta}(t) \end{pmatrix}$$

with the scaling factors k_i and the preprocessed *SpaceMouse* outputs $u_{Hci}(t)$, which already consider the deadzones around 0. These deadzones prevent undesired FU tip motions due to minimal deflections of the hand controller.

At the same time, the desired rotation around axis 7 of the MIRO $q_{7des}(t)$ is scaled up from $q_{9des}(t)$:

$$q_{7des}(t) = \psi_{des}(t) = -\frac{d_{ToothGear}}{d_{FUShaft}} q_{9des}(t).$$

The MIRO DoF 1-6 are commanded to ensure movement of the MIRO TCP (see Fig. 1) on a straight line from its position at the start of the teleoperation mode to a virtual point at (0, 0, -135 mm) in the PSU coordinate system (see Fig. 7). This virtual point is calculated in the MIRO Base coordinate system after the PSU pose was registered as described in subsection III-A.

The Arduino firmware for RSU and PSU was adapted for the additional components in *CoFlex TOP* like the inductive sensor for the tip and the encoder for the slip detection.

To measure the FU tip poses in six DoF during both the test of technical functionality and the user study, an electromagnetic tracking system *NDI Aurora* consisting of an *Aurora Tabletop Field Generator* and an *Aurora Micro 6DoF Sensor*[10] at the FU tip was used (compare Fig. 1). The system provided an update rate of 66 Hz.

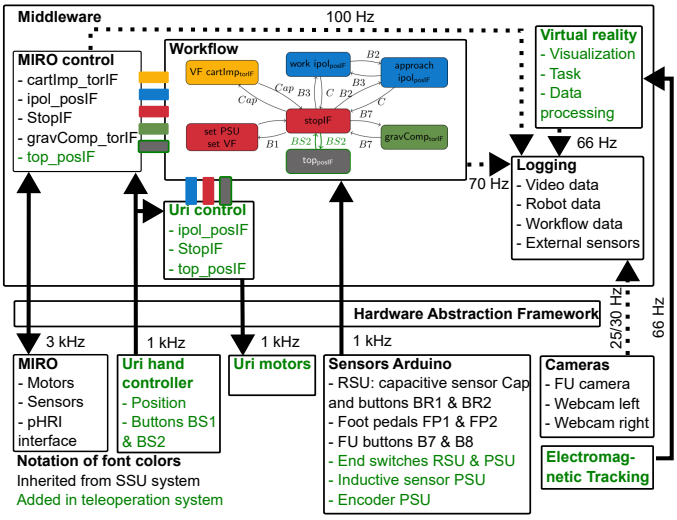

Fig. 8. The modular software architecture for the *CoFlex TOP* user study: the externally parametrized workflow is implemented as a state machine and triggers the activation of the different MIRO and Uri control modes. The Uri control communicates via a Hardware Abstraction Framework with the three Uri motors for the FU actuation. The electromagnetic tracking system sends the FU tip pose at 66 Hz to the virtual reality implementation of the user study task. The virtual reality forwards its internal data and the tracking data to the logging framework, which performs the time-synchronized acquisition of data from the different system components.

V. Results

The *CoFlex TOP* system was evaluated regarding its actuation properties and its feasibility for fine manipulation.

A. Properties of the developed system

The evaluation of the FU tip position repeatability was based on ISO 9283 [21], but adapted for 1 DoF: each motor (q_8, q_9 and q_{10}) was driven in 30 cycles to seven predefined positions while the *NDI Aurora* tracked the FU tip.

The FU tip poses for this separate variation of q_8, q_9 and q_{10} exhibited an unidirectional position repeatability of 1.41 mm for q_8, 4.62 mm for q_9 and 5.12 mm for q_{10}. All three DoFs showed hysteresis for different approach directions to the predefined positions. For the variation of q_8, also a deviation in negative x-direction of the PSU coordinate system was observed (see Fig. 9). A sensor test for the planned slip detection

[9]MathWorks, Inc., Natick, MA, USA

[10]both Northern Digital Inc., Waterloo, Canada

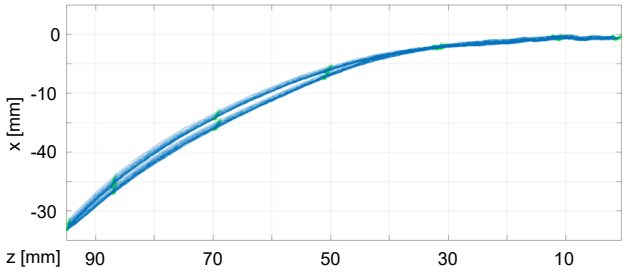

Fig. 9. FU tip movement for shaft translation in z-direction of the PSU coordinate system (displayed in Fig. 7 right).

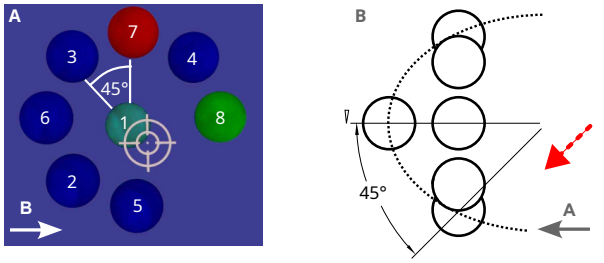

Fig. 10. Left: The virtual reality scenario as seen by the user study participants on the upper screen of the system (compare Fig. 1). They had to position the target cross in the center of the red target sphere, and press a foot pedal. Once the target was marked, it changed its color to green and one of the inactive blue spheres was marked as the new target. If one sphere was not marked within 90 s, it changed its color to turquoise and the next sphere was marked. The numbers 1 to 8 indicate the marking sequence. Right: The target spheres lied on an ellipsoid (dashed line). The red dashed arrow indicates the start pose of the FU tip.

demonstrated a position deviation of 10.0 mm between the shaft translation motor (6) and the position encoder (7) (see Fig. 7) after 60 shaft insertions and 60 shaft retractions over 100.0 mm.

B. Feasibility for fine manipulation

To compare the capability for the fine manipulation of the FU tip pose in manual FU operation and in teleoperation with *CoFlex TOP*, a user study in a virtual reality scenario was performed. The ten participants (8 male, 2 female, average age 30.1 ± 3.6 years, technical background) rated their experience with robots, on a scale of 1 = none to 10 = expert, as 6.1 ± 2.1, and their experience with FUs as 2.0 ± 1.6[11].

Within the user study, they had to move the real, electromagnetically tracked FU tip according to the virtual reality visualization displayed in Fig. 10. Eight target spheres with 10 mm diameter were placed on the surface of an ellipsoid with 60 mm length, 40 mm width and 40 mm height. The ellipsoid dimensions roughly reflect the size of a human renal pelvis. The study participants had to orientate the FU tip towards the center of each sphere in a predefined order before marking it by pressing a foot pedal. The goal communicated to the study participants was to mark the center of the target spheres as accurate as possible, not to finish the task as fast as possible. To guide them through the task, the current target sphere changed its color from blue (default color) to red. Once the participant had marked a sphere, its color changed to green and the next target was colored red. If the participant could not mark the sphere within 90 s, the sphere's color changed to turquoise and the next target was marked.

Each participant alternately performed three runs in the manual and three in the teleoperation scenario. Five participants started with the manual and five with the teleoperation scenario. The order of the target spheres within one run was the same for each run and is indicated by the numbers in Fig. 10 left (which were not visible to the study participants).

In both scenarios, the FU tip pose, the time for marking each target and the distance between marking and target center were logged. The subjective workload was inquired with the NASA-TLX [22] and the perceived usability of each scenario with the System Usability Scale (SUS) [23], [24]. In the teleoperation scenario, additionally relevant robot data (control mode, TCP pose, external forces and torques) as well as data from the FU actuation were logged.

If for the obtained quantitative values normal distribution could be confirmed using the *Shapiro-Wilk* test with a significance level of 0.05, the P value was calculated with a paired samples two-tail t-test. The results of the user study are summed up in Table I.

TABLE I
TARGET DISTANCE, TRAJECTORY LENGTH, TASK COMPLETION TIMES, NASA-TLX AND SUS VALUES FOR MANUAL FU OPERATION AND TELEOPERATION WITH *CoFlex TOP* (X = NO NORMAL DISTRIBUTION).

Run	Variable	Manual	Teleoperation	P value
1	Target distance [mm]	0.706 ± 0.713	0.553 ± 0.435	
	Trajectory length [mm]	753.8 ± 284.0	627.9 ± 152.3	0.2006
	Time [s]	125.4 ± 30.2	153.7 ± 34.5	0.0808
	NASA-TLX	50.2 ± 16.9	32.5 ± 14.0	0.0006
	SUS	60.5 ± 9.6	79.0 ± 10.0	0.0022
2	Target distance [mm]	0.620 ± 0.623	0.519 ± 0.614	
	Trajectory length [mm]	674.4 ± 227.2	580.8 ± 205.8	X
	Time [s]	126.8 ± 39.5	144.1 ± 42.3	0.0038
	NASA-TLX	37.6 ± 9.3	23.0 ± 13.1	0.0037
	SUS	63.8 ± 13.5	85.5 ± 9.3	X
3	Target distance [mm]	0.579 ± 0.595	0.445 ± 0.344	
	Trajectory length [mm]	561.1 ± 166.6	565.6 ± 122.6	X
	Time [s]	105.0 ± 23.7	135.8 ± 33.6	0.0005
	NASA-TLX	28.2 ± 10.3	26.9 ± 14.3	0.7947
	SUS	71.5 ± 15.3	82.5 ± 12.1	0.1419

VI. DISCUSSION

The system properties as well as the test results for technical functionality and for fine manipulation capabilities confirm the feasibility of *CoFlex TOP* for FU teleoperation.

A. Properties of the developed system

The developed system hardware enables quick and tool-free transitions between the three support degrees (compare the arrows in Fig. 3): from *Manual Surgery* to *Solo Surgery*, the surgeon just inserts the FU handle into the RSU shell and

[11] All participants had signed a declaration of consent before. The obtained data were made anonymous immediately after the end of the user study.

activates the impedance control by pressing a button at the robot arm. From *Solo Surgery* to *Teleoperation*, the surgeon inserts the FU tip into the ureteral access sheath, then connects the motors for the FU actuation to the FU handle lever and the flexible shaft respectively. By pressing a button at the hand controller, the telemanipulation is started[12].

As shown in Table II, the properties of *CoFlex TOP* are similar or better compared to human surgeons: The width of the PSU from the ureteral access sheath to the robot sided shaft guidance is 84.25 mm. This is comparable to the 95th percentile of hand width for women (84 mm) and below the 50th percentile of hand width for men (87 mm) [25]. Thus the same FU shaft portion can be inserted into the patient using *CoFlex TOP* as in manual fURS.

The rotation around the FU shaft axis is limited by the MIRO axis 7. The motion range of this axis is with 325° (±162.5°) larger than the on average 135° of the human wrist (60° extension/dorsiflexion towards the arm outside and 75° flexion/palmarflexion towards the arm inside) [25].

TABLE II
COMPARISON OF THE PROPERTIES OF MANUAL URETEROSCOPE ACTUATION AND OF THE *CoFlex TOP* TELEOPERATION SYSTEM.

Property	Human surgeon	*CoFlex TOP*
Width actuation unit	87 mm [25]	84.25 mm
Rotation range around FU shaft	135° [25]	325°
Translation speed insertion	48.3±64.6 mm/s [9]	max. 74.9 mm/s
Translation speed manipulation	4.4±19.2 mm/s [9]	max. 74.9 mm/s
Translation speed retraction	57.3±73.6 mm/s [9]	max. 74.9 mm/s

The PSU of *CoFlex TOP* enables a maximum shaft translation speed of 74.9 mm/s. As no information on the average shaft translation speeds during fURS was available from literature, these data were derived from the measurements of a previous user study with urology surgeons: in the robotic scenario of Task 2 in [9], five different surgeons had used the DLR MIRO in *Solo Surgery* mode to inspect the silicone models of a left and a right kidney[13] for colored pearls in the calyces. In total, 9 runs (5 left kidney, 4 right kidney) were included in the analysis[14]. Each run was distributed into three phases by manual annotation: insertion into the kidney model, manipulation within the model, and retraction from the model. Subsequently, the mean value and standard deviation of the shaft translation speed during each phase of one run were calculated. Finally, the combined mean values and standard deviations for all 9 runs were determined as displayed in Table II. The maximum shaft translation speed of *CoFlex TOP* exceeds the mean speeds in all three phases of the kidney inspection task. For the insertion and retraction phase, however, it is within the standard deviation. This seems acceptable as these phases only make up for a small portion of the overall intervention time in fURS.

The proximity of the motion trajectories (blue lines) and the measurement positions (green dots) in Fig. 9 confirms the repeatability of the translation in the mm-range. Additionally it shows a descent of the tip, due to gravity acting on the tip and the attached tracker. As even low interaction forces with the FU have such impact, an automated FU tip positioning is only possible in closed-loop control, either using electromagnetic tracking or a SLAM system [26].

The sensor test for the proposed slip detection confirms the feasibility of the concept. Its goal is the detection of slip in the mm-range between the FU shaft and the rollers. Moreover the deviation between motor position sensor and encoder can be reset to 0 regularly. Thus, the uniform increase of the deviation to 10.0 mm after a summed up motion of 6000 mm seems acceptable. Consequently, the slip detection (which was not used during the user study) will be fully integrated in the future system.

B. Feasibility for fine manipulation

The user study confirmed the feasibility of the developed teleoperation system for fine manipulation. The target distance and its standard deviation was for all three runs lower in the teleoperation scenario. However, as the values for the single targets were not normally distributed, no statistical significance could be demonstrated. The trajectory lengths and their standard deviations were lower for the teleoperation scenario in the first two runs and comparable in the third run. This indicates a more goal-oriented movement especially for less experienced users. For both scenarios, the decrease in task completion times and NASA-TLX values as well as the increase of the SUS values between Run 1 and Run 3 indicate learning effects of the participants. The SUS values of 79.0 to 85.5 confirm the good usability of the teleoperation system.

The task completion time was lower for manual FU operation than for teleoperation in all three runs. While a minimum task completion time was not the primary goal of the user study task, this nonetheless indicates improvement potentials in the teleoperation system. The longer times do not result from the virtual reality scenario as this was calculated only from the electromagnetic tracking data. The actuation of shaft translation and rotation by the PSU could have an influence, but no corresponding feedback was received from the study participants. Based on the study participants' feedback, the following improvement potentials were identified:

- **Mapping between hand controller and FU tip bending**: options for motion scaling and mapping inversion according to user preferences should be provided.
- **Stick-slip effect for FU tip bending**: this behavior impeded an accurate tip positioning in teleoperation. It relates to the deadzone and transmission function of the hand controller as well as the internal friction and hysteresis of the FU. The first problem can be solved by tuning the hand controller parameters. The second problem can be addressed by considering friction and/or hysteresis models (compare e.g. [27]) in calculating q_{10des}.

[12]The video attachment demonstrates the second transition in less than 15 s.
[13]SAMED GmbH, Dresden, Germany
[14]one right kidney run was excluded due to a robot emergency stop

C. Outlook

The presented system already integrates provisions for a slip detection of the shaft translation and a sterility concept. Its PSU can be easily modified to be waterproof against liquid flow from the ureteral access sheath by coating the slip position encoder board and using waterproof connectors. The repeated transition between manual and teleoperation mode during the user study caused no problems, confirming the principal feasibility of the hybrid surgery workflow from Fig. 4. The option for switching to *Solo Surgery* with unaltered haptic feedback from the operation site mitigates the risks due to lacking haptic feedback in *Teleoperation*.

After implementing the slip detection, sterility concept and PSU modifications and improving the telemanipulation of the FU tip (compare section VI), a more elaborate study with urology surgeons is desirable. It should focus on the usability of the system, its compatibility with the clinical workflow and its effectiveness in a clinically relevant task (e.g. a dusting task in virtual reality).

VII. Conclusion

The introduced *CoFlex TOP* system for the teleoperation of flexible ureteroscopes supports the concept of hybrid robotic surgery: the user can select between *Manual Surgery*, *Solo Surgery* and *Teleoperation*, quickly and tool-free. Adaptations to different ureteroscope models only require minor modifications of the *Robot Side Unit* and the system software. The technical evaluation of the actuation confirmed the motion ranges and speeds to be equal or larger compared to human surgeons and a sufficient position repeatability. The initial user study demonstrated the feasibility of *CoFlex TOP* for teleoperated fine manipulation of the FU tip pose.

References

[1] I. Sorokin, C. Mamoulakis, K. Miyazawa, A. Rodgers, J. Talati, and Y. Lotan, "Epidemiology of stone disease across the world," *World Journal of Urology*, vol. 35, no. 9, pp. 1301–1320, Feb. 2017.

[2] S. R. Khan, M. S. Pearle, W. G. Robertson, G. Gambaro, B. K. Canales, S. Doizi, O. Traxer, and H.-G. Tiselius, "Kidney stones," *Nature Reviews Disease Primers*, vol. 2, no. 1, Feb. 2016.

[3] C. Türk, A. Petřík, K. Sarica, C. Seitz, A. Skolarikos, M. Straub, and T. Knoll, "EAU guidelines on interventional treatment for urolithiasis," *European Urology*, vol. 69, no. 3, pp. 475–482, Mar. 2016.

[4] B. R. Matlaga, B. Chew, B. Eisner, M. Humphreys, B. Knudsen, A. Krambeck, D. Lange, M. Lipkin, N. L. Miller, M. Monga, V. Pais, R. L. Sur, and O. Shah, "Ureteroscopic laser lithotripsy: A review of dusting vs fragmentation with extraction," *Journal of Endourology*, vol. 32, no. 1, pp. 1–6, Jan. 2018.

[5] O. Traxer and E. X. Keller, "Thulium fiber laser: the new player for kidney stone treatment? A comparison with holmium:YAG laser," *World Journal of Urology*, vol. 38, no. 8, pp. 1883–1894, Feb. 2019.

[6] I. M. Tjiam, R. H. Goossens, B. M. Schout, E. L. Koldewijn, A. J. Hendrikx, A. M. Muijtjens, A. J. Scherpbier, and J. A. Witjes, "Ergonomics in endourology and laparoscopy: An overview of musculoskeletal problems in urology," *Journal of Endourology*, vol. 28, no. 5, pp. 605–611, May 2014.

[7] K. A. Healy, R. W. Pak, R. C. Cleary, A. Colon-Herdman, and D. H. Bagley, "Hand problems among endourologists," *Journal of Endourology*, vol. 25, no. 12, pp. 1915–1920, Dec. 2011.

[8] C. Schlenk, J. Klodmann, K. Hagmann, A. Kolb, A. Hellings-Kus, F. Steidle, D. Schoeb, T. Jurgens, A. Miernik, and A. Albu-Schaffer, "A robotic system for solo surgery in flexible ureterorenoscopy," *IEEE Robotics and Automation Letters*, vol. 7, no. 4, pp. 10 558–10 565, Oct. 2022.

[9] C. Schlenk, K. Hagmann, F. Steidle, L. O. Maza, A. Kolb, A. Hellings-Kuß, D. S. Schöb, J. Klodmann, A. Miernik, and A. Albu-Schäffer, "A robotic system for solo surgery in flexible ureteroscopy: development and evaluation with clinical users," *International Journal of Computer Assisted Radiology and Surgery*, Apr. 2023.

[10] C. Fang, D. Cesmeci, J. D. J. Gumprecht, E.-M. Krause, G. Strauss, and T. C. Lueth, "A motorized hand-held flexible rhino endoscope in ENT diagnoses and its clinical experiences," in *2012 4th IEEE RAS & EMBS International Conference on Biomedical Robotics and Biomechatronics (BioRob)*, IEEE, Ed., Jun. 2012, pp. 853–858.

[11] K. Olds, A. Hillel, J. Kriss, A. Nair, H. Kim, E. Cha, M. Curry, L. Akst, R. Yung, J. Richmon, and R. Taylor, "A robotic assistant for trans-oral surgery: the robotic endo-laryngeal flexible (robo-ELF) scope," *Journal of Robotic Surgery*, vol. 6, no. 1, pp. 13–18, Dec. 2011.

[12] J. G. Ruiter, G. M. Bonnema, M. C. van der Voort, and I. A. M. J. Broeders, "Robotic control of a traditional flexible endoscope for therapy," *Journal of Robotic Surgery*, vol. 7, no. 3, pp. 227–234, Apr. 2013.

[13] L. A. Zhang, R. Khare, E. Wilson, S. X. Wang, C. A. Peters, and K. Cleary, "Robotic assistance for manipulating a flexible endoscope," in *2014 IEEE International Conference on Robotics and Automation (ICRA)*, IEEE, Ed., May 2014, pp. 5380–5385.

[14] T. Iwasa, R. Nakadate, S. Onogi, Y. Okamoto, J. Arata, S. Oguri, H. Ogino, E. Ihara, K. Ohuchida, T. Akahoshi, T. Ikeda, Y. Ogawa, and M. Hashizume, "A new robotic-assisted flexible endoscope with single-hand control: endoscopic submucosal dissection in the ex vivo porcine stomach," *Surgical Endoscopy*, vol. 32, no. 7, pp. 3386–3392, Apr. 2018.

[15] D.-H. Lee, B. Cheon, J. Kim, and D.-S. Kwon, "easyEndo robotic endoscopy system: Development and usability test in a randomized controlled trial with novices and physicians," *The International Journal of Medical Robotics and Computer Assisted Surgery*, vol. 17, no. 1, pp. 1–14, Oct. 2020.

[16] M. M. Desai, R. Grover, M. Aron, A. Ganpule, S. S. Joshi, M. R. Desai, and I. S. Gill, "Robotic Flexible Ureteroscopy for Renal Calculi: Initial Clinical Experience," *Journal of Urology*, vol. 186, no. 2, pp. 563–568, Aug. 2011.

[17] J. Rassweiler, M. Fiedler, N. Charalampogiannis, A. S. Kabakci, R. Saglam, and J.-T. Klein, "Robot-assisted flexible ureteroscopy: an update," *Urolithiasis*, vol. 46, no. 1, pp. 69–77, Nov. 2017.

[18] X. Shu, Q. Chen, and L. Xie, "A novel robotic system for flexible ureteroscopy," *The International Journal of Medical Robotics and Computer Assisted Surgery*, vol. 17, no. 1, pp. 1–11, Nov. 2020.

[19] J. Zhao, J. Li, L. Cui, C. Shi, and G. Wei, "Design and performance investigation of a robot-assisted flexible ureteroscopy system," *Applied Bionics and Biomechanics*, vol. 2021, pp. 1–13, Nov. 2021.

[20] J. Park, C. H. Gwak, D. Kim, J. H. Shin, B. Lim, J. Kim, B. Cheon, J. Han, D.-S. Kwon, and H. K. Park, "The usefulness and ergonomics of a new robotic system for flexible ureteroscopy and laser lithotripsy for treating renal stones," *Investigative and Clinical Urology*, vol. 63, no. 6, p. 647, 2022.

[21] International Organization for Standardization, *ISO 9283:1998(E): Manipulating industrial robots - Performance criteria and related test methods*. Vernier, Geneva, Switzerland: International Organization for Standardization, 1998. [Online]. Available: https://www.iso.org/standard/22244.html

[22] S. G. Hart and L. E. Staveland, "Development of NASA-TLX (task load index): Results of empirical and theoretical research," in *Advances in Psychology*. North-Holland: Elsevier, 1988, vol. 52, pp. 139–183.

[23] J. Brooke, "SUS - a quick and dirty usability scale," *Usability evaluation in industry*, vol. 189, no. 194, pp. 4–7, 1996.

[24] A. Bangor, P. Kortum, and J. Miller, "Determining what individual sus scores mean: Adding an adjective rating scale," *Journal of usability studies*, vol. 4, no. 3, pp. 114–123, 2009.

[25] A. W. Wolfgang Lange, *Kleine Ergonomische Datensammlung*. TÜV Media GmbH, Köln, Sep. 2011.

[26] L. O. Maza, F. Steidle, J. Klodmann, K. Strobl, and R. Triebel, "An ORB-SLAM3-based approach for surgical navigation in ureteroscopy," *Computer Methods in Biomechanics and Biomedical Engineering: Imaging & Visualization*, pp. 1–7, 2022.

[27] T. Do, T. Tjahjowidodo, M. Lau, and S. Phee, "Adaptive control for enhancing tracking performances of flexible tendon–sheath mechanism in natural orifice transluminal endoscopic surgery (NOTES)," *Mechatronics*, vol. 28, pp. 67–78, Jun. 2015.